Letter to the Editor

Hepatic alveolar echinococcosis accompanied by lung and kidney metastases: a case description of imaging findings

Xukun Gao[1], Huaqing Tan[1], Mengdie Zhu[1], Yuxuan Wang[1], Yumeng Zhang[1], Yuntai Cao[1], Haining Fan[2]

[1]Department of Radiology, Affiliated Hospital of Qinghai University, Xining, China; [2]Department of Hepatopancreatobiliary Surgery, Affiliated Hospital of Qinghai University, Xining, China

Correspondence to: Yuntai Cao, MD. Department of Radiology, Affiliated Hospital of Qinghai University, 29 Tongren Road, Xining 810001, China. Email: caoyuntai04@126.com; Haining Fan, MD. Department of Hepatopancreatobiliary Surgery, Affiliated Hospital of Qinghai University, 29 Tongren Road, Xining 810001, China. Email: fanhaining@medmail.com.cn.

Submitted May 17, 2023. Accepted for publication Sep 21, 2023. Published online Oct 20, 2023.
doi: 10.21037/qims-23-689
View this article at: https://dx.doi.org/10.21037/qims-23-689

Introduction

Echinococcosis is a rare and neglected zoonotic disease caused by larval stages of tapeworms (cestodes) belonging to the genus *Echinococcus* (family Taeniidae). The two major species of medical and public health importance are *Echinococcus granulosus* and *Echinococcus multilocularis*, which cause cystic echinococcosis (CE) and alveolar echinococcosis (AE), respectively. Compared with CE, AE has a low incidence rate and high mortality. The annual incidence rate of CE in epidemic areas is 1–200 per 100,000, and the incidence rate of AE is 0.03–1.2 per 100,000. However, the mortality rate of untreated or improperly treated AE patients within 10–15 years of diagnosis is 90% (1). Almost all AE originate in the liver, and they can be transferred through the bloodstream to the lungs, brain, and spine, usually first to the lungs and then gradually to other organs or tissues (2,3). Hepatic alveolar echinococcosis (HAE) metastasis to the kidneys is rare. Here, we report a case of HAE metastasis to the lung and kidney successively with imaging manifestations and features to help the diagnosis of metastatic renal AE in the future and to promote early detection and treatment.

Case presentation

On 23 March 2017, a 49-year-old woman attended the Department of Hepatological Surgery at the Qinghai University Affiliated Hospital due to discomfort and pain in her lower back. Imaging at our hospital suggested HAE with intrapulmonary metastases (*Figures 1*,*2A*). Since the patient's alpha-fetoprotein (AFP) test was negative and no hydatid serological IgG enzyme-linked immunosorbent assay (ELISA) was performed, based on the imaging findings, the clinician considered her to have HAE with lung metastasis and did not exclude a liver tumor. The patient was not treated with medication (albendazole) because the condition was so severe that the clinician did not think medicine would help. From 2018 to 2019, the patient underwent a follow-up examination at our hospital and showed an increase in liver and lung lesions (*Figure 2B*,*2C*). In May 2020, the patient underwent liver transplantation and resection of an intrapulmonary lesion due to the gradual enlargement of the lesions in other hospitals and was diagnosed with HAE with lung metastasis. Unfortunately, specific clinical information was not available to us. On 15 August 2022, the patient again visited our hospital with intermittent pain in the left lumbar region. The patient had no gross hematuria, pyuria, difficulty urinating, no pain in urination, frequent urination, or urgency. Physical examination revealed the following: slight percussion pain in the left kidney area, no eminence in both kidney areas symmetrically, no localized skin redness, no rupture, no palpable mass, and no pressure pain in the ureteral pathway. Double kidney ultrasound showed hypoechoic nodules in the left kidney; abdominal computed tomography (CT) scan showed a mid-density mass shadow in the middle of the left kidney, with a size of approximately 5.50 cm × 3.80 cm, circular low-density shadow could be seen inside, and no significant

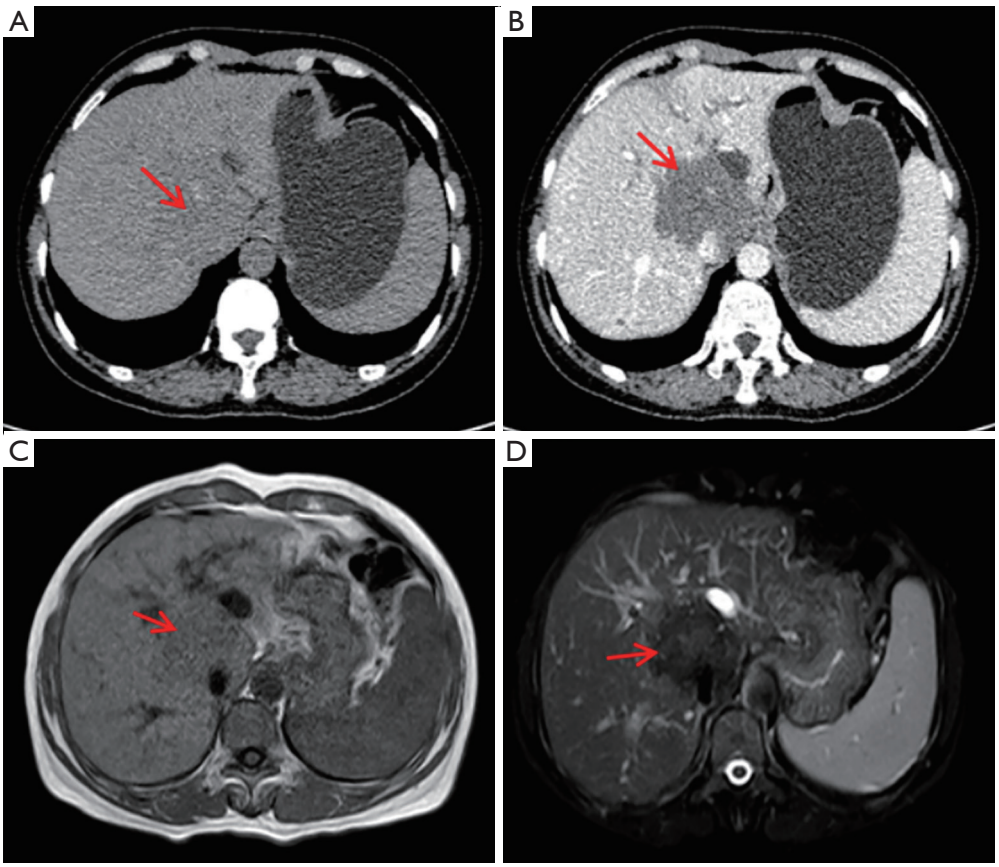

Figure 1 Diagnostic image of the patient with HAE in March 2017. (A,B) Abdominal CT scan showed a slightly low-density mass shadow resembling a circular shape in the secondary porta of the liver, with a size of approximately 5.83 cm × 5.10 cm, accompanied by punctate calcification (red arrow); enhanced scanning showed no significant enhancement (red arrow). The lesion shows hypointensity on T1WI (C) and on T2WI (D) (red arrow). HAE, hepatic alveolar echinococcosis; CT, computed tomography; T1WI, T1-weighted imaging; T2WI, T2-weighted imaging.

enhancement was observed in the enhanced scan of the lesion; Bilateral renal computed tomography angiography (CTA) showed that the left renal artery supplied the lesion; magnetic resonance imaging (MRI) showed a mass shadow in the left kidney, with unclear boundaries and a size of approximately 5.06 cm × 3.80 cm, T1-weighted imaging (T1WI) showed slight hyperintensity, with multiple cystic low signal areas visual inside. T2-weighted imaging (T2WI) mainly showed a slightly low signal, with many high cystic signals and short lines with hypointensity visible inside. Diffusion-weighted imaging (DWI) showed equal or slightly higher signal; apparent diffusion coefficient (ADC) image showed heterogeneous signal; enhanced scanning showed no significant enhancement (*Figures 2D*,*2E*,*3*). Additionally, the patient's hydatid serological IgG ELISA was positive. Based on the patient's medical history, we considered that the patient's disease was HAE with renal metastasis, and renal tumor was not excluded. On 29 August 2022, the patient underwent laparoscopic radical resection of the left kidney and tumor combined with perirenal adhesiolysis in our hospital. Postoperative macroscopic observation revealed the following: Left renal tissue removed, volume 9 cm × 6.5 cm × 5 cm, with a visible ureteral stump, 4 cm long and 0.4–0.5 cm in diameter; dissected along the contralateral side of the renal hilum, a greyish-yellow area measuring 5 cm × 4.5 cm × 4 cm was visible adjacent to the renal capsule, clearly demarcated from the surrounding tissue, with a perirenal fat volume of approximately 5 cm × 5 cm × 2 cm; pathological diagnosis: left renal AE with necrosis (*Figure 4*). It was confirmed that this case is HAE accompanied by pulmonary and renal metastasis. The patient had been taking albendazole postoperatively.

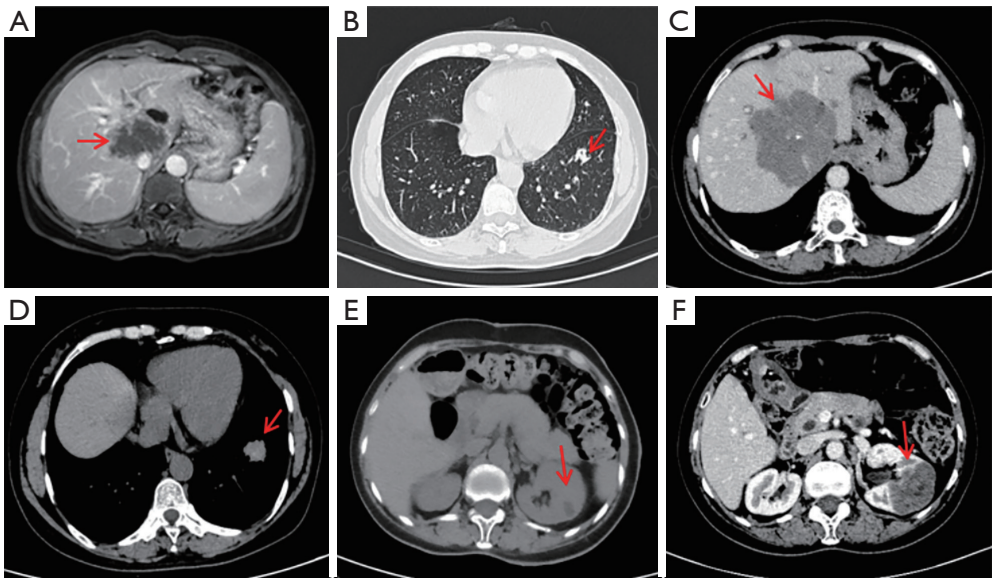

Figure 2 Diagnostic image of the patient with hepatic, pulmonary, and renal alveolar echinococcosis. (A) The enhanced MRI scan showed no significant enhancement of the lesion; the lesion encircles the intrahepatic segment of the inferior vena cava, and the lumen of the proximal parts of the left, middle, and right hepatic veins is narrowed (red arrow). (B) CT shows that the slight lobulation nodule in the lower lobe of the left lung is caused by primary liver metastasis, with a diameter of approximately 1.16 cm (red arrow). (C,D) In 2019, the patient's CT images showed significant enlargement of intrahepatic and pulmonary lesions; their sizes were approximately 8.07 cm × 8.12 cm and 2.39 cm × 2.45 cm, respectively (red arrow). (E,F) On 15 August 2022, the CT image of the patient's left kidney lesion showed no significant enhancement on the enhanced scan (red arrow). MRI, magnetic resonance imaging; CT, computed tomography.

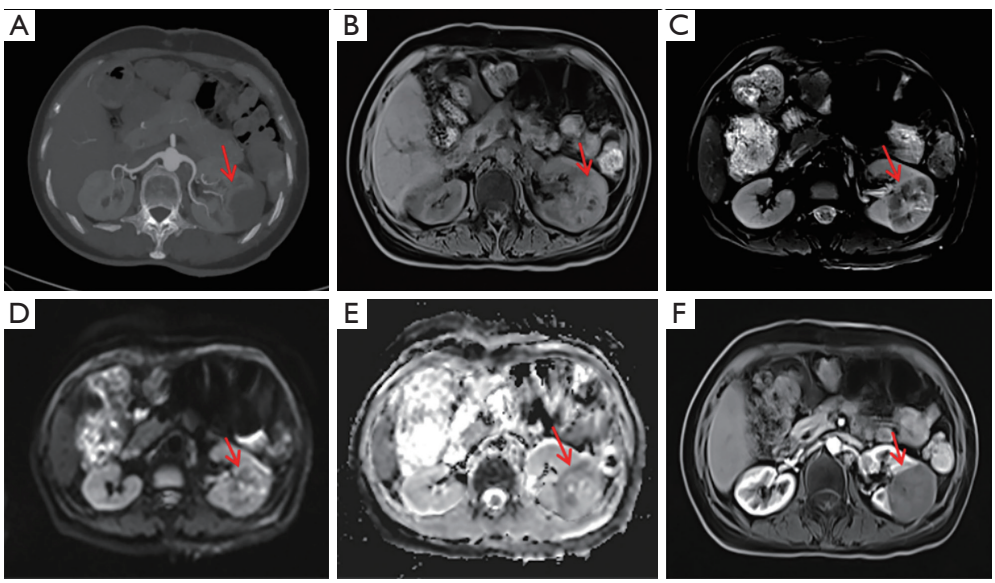

Figure 3 Diagnostic image of the patient with renal AE. (A) Bilateral renal CTA showed that the left renal artery supplied the lesion (red arrow). (B) On the T1WI, the left kidney is mainly high signal, with cystic hypointensity visible inside (red arrow). (C) On T2WI, the left kidney is mainly hypointensity with cystic high signal visual inside (red arrow). (D) DWI showed equal or slightly higher signals (red arrow). (E) The ADC image showed heterogeneous (red arrow). (F) MRI enhancement scan showed no significant enhancement of the left kidney lesion (red arrow). AE, alveolar echinococcosis; CTA, computed tomography angiography; T1WI, T1-weighted imaging; T2WI, T2-weighted imaging; DWI, diffusion-weighted imaging; ADC, apparent diffusion coefficient; MRI, magnetic resonance imaging.

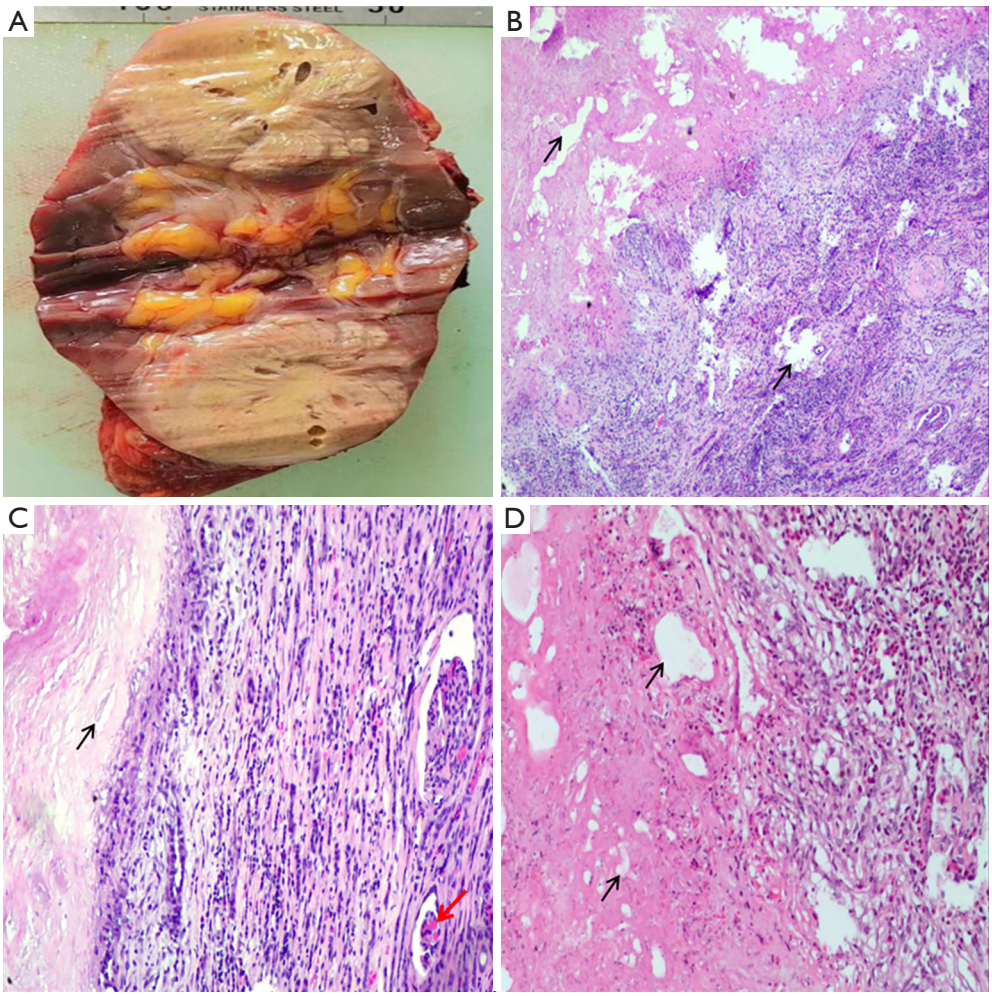

Figure 4 Postoperative specimen of left renal alveolar hydatid cyst. (A) A greyish-yellow area measuring 5 cm × 4.5 cm × 4 cm was visible adjacent to the renal capsule, clearly demarcated from the surrounding tissue. (B-D) Surgical specimen showed the AE exhibited a vesicular structure with vesicles of varying size and shape. HE staining (black arrow). The magnification of the objective lens is respectively ×40, ×100, and ×200. Ovular nodules can be seen (C, red arrow). AE, alveolar echinococcosis; HE, hematoxylin-eosin.

There were no discomfort symptoms for the patient at the 2-week, 3-month, and 6-month follow-ups. All procedures performed in this study were in accordance with the ethical standards of the institutional and national research committee(s) and with the Helsinki Declaration (as revised in 2013). Written informed consent was provided by the patient for publication of this case report and accompanying images. A copy of the written consent is available for review by the editorial office of this journal.

Discussion

AE is caused by *Echinococcus multilocularis*, the life cycle of which includes intermediate hosts in small rodents and final hosts in wild or domestic canids such as red or arctic foxes, jackals, wolves, or dogs. Humans are aberrant intermediate hosts, acquiring infection by ingesting eggs excreted in the feces of the final host (4). AE is a severe disease that causes high mortality rates, a massive economic burden, and an enormous public health burden in Asia, especially in the Qinghai-Tibet Plateau region. AE is ranked the most important species in the assessment of important food-borne parasites in Europe, with the second highest mortality rate; it is also known as "worm cancer" because it mimics the growth of malignant tumors and proliferates in a silent, infiltrative manner (4,5). Imaging is an essential tool in the

diagnosis of echinococcosis. CT is helpful in identifying the exact location, number, and size of lesions and their relationship to adjacent tissues and is highly sensitive to calcifications; MRI is more beneficial for visualizing the nature of the lesion and the surrounding vascular invasion, so CT and MRI are often applied for preoperative evaluation (6). Serological and immunological diagnoses occasionally result in false negative results, so they are only used as a reference in the diagnosis of echinococcosis (7). We report a case of primary hepatic alveolar hydatid that metastasized successively to the lungs and kidneys, with complete imaging data, from which we have analyzed the relevant features to provide some assistance in future clinical diagnosis.

Kodama *et al.* reported the MRI presentation and characteristics of 35 cases of HAE and classified them into 5 types: type I is multiple small vesicles without a solid mass; type II is multiple small vesicles with a solid mass; type III is a solid component surrounding a large and/or irregular cyst with multiple small vesicles; type IV is a solid mass without small vesicles; type V is a large vesicle without a solid mass; the lesion is predominantly low signal on both T1WI/T2WI, with small vesicles showing a high signal on T2WI and mildly enhancing at the edges of the lesion after enhancement (8). Yu *et al.* reported that the basic CT signs of HAE include a heterogeneous and substantial mass with unremarkable enhancement on enhanced scans; characteristic features include vesicular signs, calcified foci, central liquefied necrosis or cavities (9). The imaging presentation of this case was consistent with HAE type III, as proposed by Kodama *et al.* Small cysts could be seen within the solid component. In addition, foci of calcification could be seen on CT images in this case. HAE involves the lungs most commonly; the clinical signs are usually dyspnea, chest pain, and cough. About 1/3 of patients with pulmonary involvement are asymptomatic; in this case, the patient also had no clinical signs of chest at the initial diagnosis (10). The typical imaging picture of pulmonary AE is a single or multiple irregular nodular shadows in the lung with calcifications, eccentric cavities, small vacuoles, and gravelly calcifications in the center of the pulmonary AE lesion, which can be called "target sign" (11). In this case, a superficial lobulated nodule with small vacuoles in the lower lobe of the left lung was seen, consistent with the above imaging findings. Based on imaging findings, the European Network for Concerted Surveillance of Alveolar Echinococcosis and the World Health Organization (WHO) Group on Echinococcosis proposed a clinical classification for AE. It was designated as PNM classification system (P = parasitic mass in the liver, N = involvement of neighboring organs, and M = metastasis) (12,13). The lesion in our patient's liver encircled the intrahepatic segment of the inferior vena cava, narrowing the lumen of the left, middle, and right hepatic veins and metastasizing to the lungs; it can be classified as P4N1M1 according to the PNM system. The proposal of this classification can facilitate effective communication between clinicians to formulate the best treatment plan.

Case of renal metastases from HAE is scarce. Previous literature has reported AE originating in the kidney. The relevant CT scan will show a multilocular cystic lesion with typical septa and "ribbons sign". On T2WI, it will show mixed signals, with multiple smaller peripheral cysts visible; enhanced scanning will show mild enhancement of the lesion wall, cyst wall, and septum (14-16). In this case, the lesion that metastasized to the kidney appeared as an isodense shadow with a predominantly solid component on CT, which could easily be misdiagnosed as a renal neoplastic lesion without our knowledge of the patient's medical history; through enhanced scanning, we found that the lesion was not significantly enhanced and small vesicles were visible. MRI showed a solid mass shadow, with small vesicles and short-line low signal areas visible inside. In this case, the enhancement method is inconsistent with common renal tumor lesions. Therefore, when we suspect renal AE, the diagnosis should be made by combining the patient's previous history of primary liver disease and the enhancement mode of the lesion. This case had undergone pathology to support our initial diagnostic results. Furthermore, in the treatment of echinococcosis, AE can be cured by radical surgery. Patients who are no longer suitable for radical surgery due to late diagnosis can be managed with lifelong treatment with albendazole (4). Our patient underwent laparoscopic radical resection of the left kidney and tumor and took albendazole postoperatively. There was no disease recurrence at 2 weeks, 3 months, and 6 months of follow-up; she is still being followed up.

Renal AE needs to be differentiated from substantial renal tumors such as renal cell carcinoma (renal clear cell carcinoma, papillary renal cell carcinoma, chromophobe renal cell carcinoma), renal oncocytoma, and renal pelvis carcinoma. Renal clear cell carcinoma: due to the rich blood supply and short circulation time of the tumor, the solid portion of the mass appears to be significantly enhanced in the cortical phase and rapidly decreases in the medullary phase, showing the typical "fast-in, fast-out" feature on CT

or MRI enhancement scans. Papillary renal cell carcinoma: CT-enhanced scans show a low degree of enhancement of the solid part of the mass in the cortical phase, which is significantly lower than that of the renal cortex, with a tendency to increase the degree of enhancement in the subsequent phase, showing a "slow rise"; MRI-enhanced scans show a predominantly mild enhancement of the lesion, with a gentle progression from the cortical phase to the excretory phase, and a slow decrease in enhancement. Chromophobe renal cell carcinoma: CT enhanced scan shows more obvious enhancement in the parenchymal phase of the tumor compared to the cortical phase. When the tumor is large, it can appear as a "spoke-like" enhancement, and a characteristic central scar can appear in the center of the lesion; MRI enhancement scans show mild to moderate enhancement of the lesion and "spoke-like" enhancement in the excretory phase (17). Eosinophilic adenoma of the kidney: CT-enhanced scans show markedly homogeneous enhancement of the parenchymal portion of the lesion in the corticomedullary phase, with decreasing enhancement in the excretory phase, below the surrounding renal cortex. Zhang *et al.* studied renal cell carcinoma and renal eosinophilic tumor in terms of the degree of enhancement on enhanced scans (18). Their findings were as follows: in the parenchymal phase, renal clear cell carcinoma and renal eosinophil tumor have a higher degree of enhancement, renal suspicious cell carcinoma is moderately enhanced, and papillary renal cell carcinoma is less enhanced. In the excretory phase, there is more overlap in the degree of enhancement between different renal cell carcinomas. No significant enhancement on CT and MRI enhancement scans for renal AE. In contrast, renal cell carcinoma and renal eosinophilic adenoma have varying degrees of enhancement on CT and MRI enhancement scans. Therefore, it is more significant to identify them on enhanced scans. The CT manifestation of renal pelvis cancer is a soft tissue density mass shadow in the renal pelvis. When the renal pelvis and calyces are obstructed, hydronephrosis can appear. The enhanced scan of the mass shows mild to moderate enhancement, and the delayed scan can distinctly display the filling defect caused by the tumor when the remaining renal pelvis and calyces are significantly enhanced. In addition, the typical clinical presentation of renal pelvic cancer is total painless hematuria and often stones, all of which can be distinguished from renal AE.

In conclusion, metastatic renal vesicular encapsulation is very rare. By summarizing the imaging presentation of this case, we have provided important imaging evidence for the accurate preoperative diagnosis of the patient and a vital basis for selecting a reasonable treatment.

Acknowledgments

Funding: This work was supported by the National Natural Science Foundation of China (No. 82260346), Qinghai Province "Kunlun Talents High-end Innovation and Entrepreneurial Talents" Top Talent Cultivation Project (No. 13,2021), and Qinghai Provincial Department of science and technology of China (No. 2023-ZJ-918M).

Footnote

Conflicts of Interest: All authors have completed the ICMJE uniform disclosure form (available at https://qims.amegroups.com/article/view/10.21037/qims-23-689/coif). The authors have no conflicts of interest to declare.

Ethical Statement: The authors are accountable for all aspects of the work in ensuring that questions related to the accuracy or integrity of any part of the work are appropriately investigated and resolved. All procedures performed in this study were in accordance with the ethical standards of the institutional and/or national research committee(s) and with the Helsinki Declaration (as revised in 2013). Written informed consent was provided by the patient for publication of this case report and accompanying images. A copy of the written consent is available for review by the editorial office of this journal.

References

1. Wen H, Vuitton L, Tuxun T, Li J, Vuitton DA, Zhang W, McManus DP. Echinococcosis: Advances in the 21st Century. Clin Microbiol Rev 2019;32:e00075-18.
2. Liu C, Fan H, Ge RL. A Case of Human Hepatic Alveolar Echinococcosis Accompanied by Lung and Brain

Metastases. Korean J Parasitol 2021;59:291-6.
3. Atalan G, Sivrioglu AK, Sönmez G, Celik M, Simsek B. A Case of Alveolar Echinococcosis Presenting as Cerebral and Spinal Intradural Metastases. Eurasian J Med 2016;48:149-52.
4. Casulli A, Barth TFE, Tamarozzi F. Echinococcus multilocularis. Trends Parasitol 2019;35:738-9.
5. Woolsey ID, Miller AL. Echinococcus granulosus sensu lato and Echinococcus multilocularis: A review. Res Vet Sci 2021;135:517-22.
6. Liu W, Delabrousse É, Blagosklonov O, Wang J, Zeng H, Jiang Y, Wang J, Qin Y, Vuitton DA, Wen H. Innovation in hepatic alveolar echinococcosis imaging: best use of old tools, and necessary evaluation of new ones. Parasite 2014;21:74.
7. Yousofi Darani H, Jafari R. Renal echinococcosis; the parasite, host immune response, diagnosis and management. J Infect Dev Ctries 2020;14:420-7.
8. Kodama Y, Fujita N, Shimizu T, Endo H, Nambu T, Sato N, Todo S, Miyasaka K. Alveolar echinococcosis: MR findings in the liver. Radiology 2003;228:172-7.
9. Yu XK, Zhang L, Ma WJ, Bi WZ, Ju SG. An Overview of Hepatic Echinococcosis and the Characteristic CT and MRI Imaging Manifestations. Infect Drug Resist 2021;14:4447-55.
10. Aydin Y, Ogul H, Topdagi O, Ulas AB, Sade R, Ozturk G, Korkut E, Aksungur N, Sener E, Kesmez Can F, Araz O, Alper F, Eroglu A. Relevance of Pulmonary Alveolar Echinococcosis. Arch Bronconeumol (Engl Ed) 2020;56:779-83.
11. Kantarci M, Bayraktutan U, Karabulut N, Aydinli B, Ogul H, Yuce I, Calik M, Eren S, Atamanalp SS, Oto A. Alveolar echinococcosis: spectrum of findings at cross-sectional imaging. Radiographics 2012;32:2053-70.
12. Kern P, Wen H, Sato N, Vuitton DA, Gruener B, Shao Y, Delabrousse E, Kratzer W, Bresson-Hadni S. WHO classification of alveolar echinococcosis: principles and application. Parasitol Int 2006;55 Suppl:S283-7.
13. Brunetti E, Kern P, Vuitton DA; . Expert consensus for the diagnosis and treatment of cystic and alveolar echinococcosis in humans. Acta Trop 2010;114:1-16.
14. Mladenov B, Dorosiev E. Primary renal echinococcosis - a rare location of hydatid disease. Folia Med (Plovdiv) 2021;63:591-4.
15. Hamed Al Taei T, Ali Al Mail S, Hajjaj Al Thinayyan A, Alsetrawi A. Renal hydatid cyst: A case report. Radiol Case Rep 2022;17:2063-6.
16. Ishimitsu DN, Saouaf R, Kallman C, Balzer BL. Best cases from the AFIP: renal hydatid disease. Radiographics 2010;30:334-7.
17. Sun MR, Ngo L, Genega EM, Atkins MB, Finn ME, Rofsky NM, Pedrosa I. Renal cell carcinoma: dynamic contrast-enhanced MR imaging for differentiation of tumor subtypes--correlation with pathologic findings. Radiology 2009;250:793-802.
18. Zhang J, Lefkowitz RA, Ishill NM, Wang L, Moskowitz CS, Russo P, Eisenberg H, Hricak H. Solid renal cortical tumors: differentiation with CT. Radiology 2007;244:494-504.

Cite this article as: Gao X, Tan H, Zhu M, Wang Y, Zhang Y, Cao Y, Fan H. Hepatic alveolar echinococcosis accompanied by lung and kidney metastases: a case description of imaging findings. Quant Imaging Med Surg 2024;14(1):1208-1214. doi: 10.21037/qims-23-689

